

A Kinetic Analysis of DNA-Deoxy Guanine Adducts in the Nasal Epithelium Produced by Inhaled Formaldehyde in Rats—Assessing Contributions to Adduct Production From Both Endogenous and Exogenous Sources of Formaldehyde

Jerry L. Campbell Jr,^{*,1} P. Robinan Gentry,[†] Harvey J. Clewell III,^{*} and Melvin E. Andersen[‡]

^{*}Department of Health and Safety, Ramboll US Corporation, Raleigh, North Carolina 27612 [†]Department of Health and Safety, Ramboll US Corporation, Monroe, Louisiana 71201; and [‡]Andersen ToxConsulting LLC, Denver, North Carolina 28037

ABSTRACT

Although formaldehyde is a normal constituent of tissues, lifetime inhalation exposures at 6 h/day, 5 days/week at concentrations ≥ 6 ppm caused a nonlinear increase in nasal tumors in rats with incidence reaching close to 50% at 15 ppm. Studies with heavy isotope labeled [¹³CD₂]-formaldehyde permit quantification of both the mass-labeled exogenous and endogenous DNA-formaldehyde reaction products. An existing pharmacokinetic model developed initially to describe ¹⁴C-DNA-protein crosslinks (DPX) provided a template for describing the time course of mass-labeled adducts. Published datasets included both DPX and N₂-HO¹³CD₂-dG adducts measured after a single 6-h exposure to 0.7, 2, 6, 9, 10, or 15 ppm formaldehyde, after multi-day exposures to 2 ppm for 6 h/day, 7 days/week with interim sacrifices up to 28 days, and after 28-day exposures for 6 h/day, 7 days/week to 0.3, 0.03, or 0.001 ppm. The existing kinetic model overpredicted endogenous adducts in the nasal epithelium after 1-day [¹³CD₂]-formaldehyde exposure, requiring adjustment of parameters for rates of tissue metabolism and background formaldehyde. After refining tissue formaldehyde parameters, we fit the model to both forms of adducts by varying key parameters and optimizing against all 3 studies. Fitting to all these studies required 2 nonlinear pathways—one for high-exposure saturation of clearance in the nasal epithelial tissues and another for extracellular clearance that restricts uptake into the epithelial tissue for inhaled concentrations below 0.7 ppm. This refined pharmacokinetic model for endogenous and exogenous formaldehyde acetal adducts can assist in updating biologically based dose-response models for formaldehyde carcinogenicity.

Key words: biotransformation; toxicokinetics; pharmacokinetics.

Formaldehyde is a ubiquitous environmental contaminant. Ambient air concentrations in the United States are on the order of 3 ppb (parts per billion; USEPA 2010), while average indoor air concentrations are typically in the 16–32 ppb range (Salthammer et al., 2010). Inhalation of formaldehyde caused nasal cancer in rats exposed for 2 years to concentrations of

6 ppm (ie, 6000 ppb) and above. In addition, formaldehyde is an endogenous metabolite of various cellular reactions and present in cells in a hydrated form, formaldehyde hydrate or formaldehyde acetal (FA). Cellular FA reversibly reacts with various nucleophiles, such as glutathione (GSH), and various macromolecules. Estimates of the concentration of cellular FA rely on

methods that convert free FA to stable reaction products—methods that result in a combined measurement of both free and reversibly bound FA. A significant challenge with FA risk assessments is to account for the presence of endogenous FA and assess whether there are significant differences in toxicokinetics of intracellularly produced FA versus inhaled FA.

The earliest pharmacokinetic (PK) analyses of FA-DNA reaction products (Heck and Casanova, 1999) focused on the time course and concentration dependent formation of radiolabelled ^{14}C -DNA-protein crosslinks (DPX) following formaldehyde inhalation. The results from this analysis provided dose-response curves that passed through the origin on the curve relating ^{14}C -DPX concentration with inhaled radiolabeled formaldehyde. These curves were inadvertently misleading, giving the false impression that there would be no DPX in the absence of exposure. Although there were no ^{14}C -DPX, there should be endogenous DPX in the cells due to the background FA produced by cellular metabolism. A subsequent effort extended the DPX PK model of Heck and Casanova (1999) and was designed to simulate concentrations of both endogenous and exogenous DPX (Andersen et al., 2010). The main goal of this second model was to demonstrate that descriptions of DPX that accounted for cellular production and metabolism of FA could also provide estimates of endogenous DPX, including background DPX level in the absence of any exogenous exposure. In this expanded PK model, all FA, whether formed from inhaled exogenous FA or endogenously produced FA, entered a common cellular pool, that is, FA from both sources was equally available for metabolism, interaction with nucleophiles, and formation of DNA reaction products. This PK model for FA disposition in nasal epithelial cells was designed to examine the kinetic basis of the nonlinear increase of DPX observed in the nasal tissue of rodents exposed to FA in air, and to demonstrate that endogenous DPX concentrations would also have a background concentration in the absence of formaldehyde exposure. However, at the time the Andersen et al. (2010) model was under development, no data on background DPX concentrations were available to assess basal levels and test the accuracy of model predictions for concentrations of FA-DNA reaction products following various formaldehyde exposures.

The technologies for assessing concentrations of various DNA adducts have now progressed, providing the opportunity to assess background adduct concentrations independent of those produced by inhalation. Lu et al. (2010, 2011) and Yu et al. (2015) found significant amounts of FA-reaction products, N(2)-hydroxymethyl-dG monoadducts and dG-dG cross-links, in nonexposed rats and primates. Both time course and dose-response studies are now available on the differential dose-response of endogenous and exogenous FA-DNA reaction products. Although adducts from inhaled exogenous formaldehyde (ie, from ^{13}C and ^2H dual labeled formaldehyde) increased in a nonlinear manner with increasing exposure, adducts with endogenously produced formaldehyde did not change appreciably from background across the exposure ranges evaluated. There are also more recent studies at 0.3 ppm, ie, at concentrations below the exposures used in the cancer bioassays, where no increases in adducts were observed (Leng et al., 2019). Our goal here was to adapt the PK model for formaldehyde PKs developed for DPX (Andersen et al., 2010) and describe the production of both endogenous and exogenous FA-DNA reaction products (eg, adducts) for a diverse suite of studies at inhaled concentrations from 0.001 to 15 ppm. Another contribution of the modeling was to assess whether descriptions with a single well-mixed cellular FA compartment could describe adduct formation from

formaldehyde produced both by endogenous cellular metabolism and delivered exogenously by inhalation.

MATERIALS AND METHODS

Kinetic data. Datasets from studies conducted by Leng et al. (2019), Lu et al. (2010, 2011), and Yu et al. (2015) were used in parameterizing the PK model for simulating dG-bound FA and are summarized in Supplementary Table 1. Lu et al. (2010) reported levels of endogenous and exogenous dG-bound FA in nasal tissue of rats exposed for either 1 or 5 days to 10 ppm ^{13}C and ^2H dual labeled FA. In a subsequent paper, Lu et al. (2011) reported the levels of dG-bound FA in rat nasal tissue after a single 6-h exposure to 1, 2, 6, 9, or 15 ppm labeled FA. Yu et al. (2015) investigated the time-course for dG binding of FA in rat nasal tissue after exposure to 2 ppm FA for up to 28 consecutive days. Data were reported at the end of exposure on days 7, 14, 21, and 28. Kinetic data to inform the clearance/repair of dG-bound FA were reported for 6, 24, 72, and 168 h postexposure. In the Leng et al. (2019) study, no formaldehyde DNA reaction products were detected following exposures to low concentrations (300, 30, or 1 ppb). The data reported in these studies were also used in developing a parameter set that accounted for formaldehyde-DNA reaction products across the full range of the concentrations evaluated.

PK modeling. The PK model developed here for formaldehyde dG adducts is based on the previously developed models for formaldehyde DPX (Andersen et al., 2010; Conolly et al., 2000). In the model for dG adducts (Figure 1), as in the Andersen et al. (2010) DPX model, inhaled formaldehyde rapidly hydrates, forming FA ($\text{CH}_2(\text{OH})_2$). The FA is lost (K_{21}) by reaction with cellular components and by diffusion back to the air phase or into deeper tissues. Alternatively, FA conjugates (K_{23}) with GSH to form formaldehyde GSH thioacetal (FSG: $\text{CH}_2(\text{OH})(\text{SG})$). FSG can add water, releasing FA (K_{32}), or be converted enzymatically by formaldehyde dehydrogenase to formic acid (V_{max}/K_m), with the release of GSH. In the current adduct model, free FA is the sole source of DNA adducts (K_{dna}). Adducts are repaired with a rate constant, K_{rep} , a step that releases free FA. However, our dG adduct model differs from the DPX model of Andersen et al. (2010) in that it uses measured tissue volumes to define the nasal region of interest (Conolly et al., 2000; Gross et al., 1982) in order to be consistent with the nasal respiratory epithelial region that was harvested in the experimental studies (Leng et al., 2019; Lu et al., 2010, 2011; Yu et al., 2015). In our initial parameterization of the current model structure comparing model predictions with the results from dG-binding studies, we used data for endogenous dG-FA adduct concentrations and the estimated dG-FA adduct half-life of 7 days (Yu et al., 2015) to visually the rate constants, K_{dna} and K_{rep} (for production and repair of the dG-FA adducts). All other initial estimates of parameters were retained from the DPX model (Andersen et al., 2010).

In addition to the PK model for cellular metabolism, terms for possible clearance of inhaled formaldehyde prior to cellular uptake were also evaluated. This possibility was described by adding either a saturable (equation 1) or a zero order (equation 2) clearance process restricting uptake from the air phase into the tissue compartment:

$$\text{uptake} = (C_{\text{inh}} * QP - (V_{\text{max}}M_{\text{uc}} * C_{\text{inh}})/(K_mM_{\text{uc}} + C_{\text{inh}})) \quad (1)$$

$$\text{uptake} = (C_{\text{inh}} * QP - \text{VMMUC}) \quad (2)$$

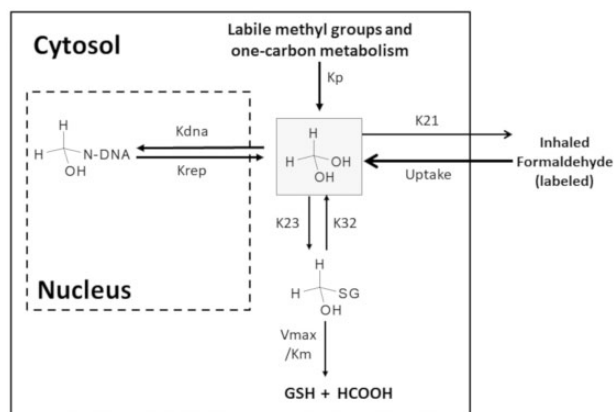


Figure 1. Pharmacokinetic model for formaldehyde adducts. In the model, inhaled formaldehyde is rapidly hydrated, forming formaldehyde acetal (FA: $\text{CH}_2(\text{OH})_2$). The FA is lost (K_{21}) by reaction with cellular components and by diffusion back to the air phase or into deeper tissues. Alternatively, FA can be conjugated (K_{23}) to glutathione (GSH) to form formaldehyde GSH thioacetal (FSG: $\text{CH}_2(\text{OH})(\text{SG})$). FSG can add water, releasing FA (K_{32}), or be converted by formaldehyde dehydrogenase to formic acid (V_{max}/K_m), with the release of GSH. The model assumes that only FA is a source of DNA adducts (K_{dna}), which can then be repaired, releasing FA (K_{rep}).

C_{inh} is the inhaled concentration of formaldehyde (mM); Q is the ventilation rate (l/h); $V_{\text{max}}M_{\text{uc}}$ is the maximum rate of extracellular formaldehyde clearance (mg/h) and K_mM_{uc} is the affinity constant for the extracellular clearance pathway (mg/l). The zero-order extracellular clearance represents the limit when K_mM_{uc} is extremely small (high affinity). The result of this assumption would be that up to a flux of $V_{\text{max}}M_{\text{uc}}$, no inhaled formaldehyde moves through the extracellular tissues to the epithelial cells themselves.

Parameter optimization. The overall approach to model development and parameter estimation is shown in Figure 2. After initial test, the 7.1-day half-life which was driven by the final data point in the Yu study, proved too slow to allow both the single-day concentration response and 28 days repeated exposure to be fit without appreciable change to endogenous bound FA in both scenarios (data not shown). K_{rep} was visually adjusted until both datasets could be reasonably fit without appreciable change to the endogenous dG-FA. The final value for K_{rep} was 0.0063 h^{-1} corresponds to a half-life of 5 days. Parameter estimation was performed by minimizing the sum of squares error between natural log of the simulation and measured exogenous dG-bound FA in an iterative process. Starting with the parameters from Andersen et al. (2010), K_{dna} and the initial concentrations of background endogenous adduct levels (AENDDG0), endogenous FA (AFA0), and endogenous FA bound to GSH (ASG0) were fixed to maintain steady state across the Lu et al. (2011) concentration response (ie, flat response across all concentrations) in the absence of exogenous FA. K_{21} , V_{max} , and K_{dna} were then optimized to the adduct data reported in rat nasal tissue following 6-h exposures ranging from 1 to 15 ppm FA (Lu et al., 2011). The endogenous production rate (K_p) and the initial states were then set to the endogenous data reported by Lu et al. (2011). K_{21} , V_{max} , and K_{dna} were then reoptimized. There were no parameters changed to fit the Yu et al. 28-day repeated exposure to 2 ppm. After developing a parameter suite that described the studies at 0.7 ppm and above, the model was then used to assess VMMUC to provide consistency with the nondetect levels for adducts reported for rat tissues following exposure to

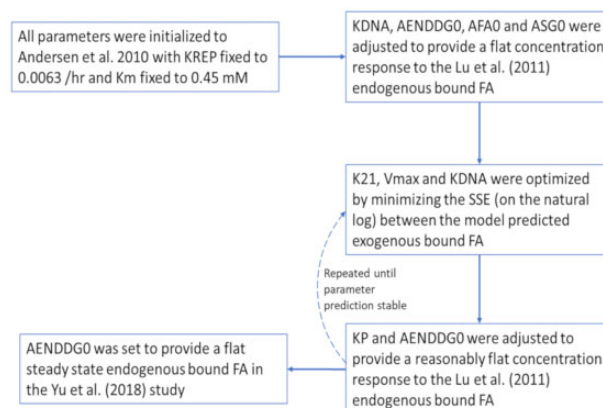


Figure 2. Approach used to re-fit the formaldehyde acetal (FA) model parameters in the FA pharmacokinetic model to account for endogenous and exogenous $\text{N}_2\text{-HO}^{13}\text{CD}_2\text{-dG}$ adducts.

0.3 ppm (Leng et al., 2019). To do this, VMMUC was visually estimated to provide an exogenous dG-FA binding that was slightly below with the limit of detection reported by Leng et al. (2019).

Software and packages. The optimization was undertaken with the nloptr reimplement of the Subplex algorithm (NLOPT_LN_SBPLX) which is a variant of the Nelder-Mead algorithm. All simulations were conducted in R. Specifically, the model was written in MCSim (ver. 5.6.6, Bois 2009), translated to C and then compiled (Rtools, Ver. 3.3.0.1959) in R (Ver. 3.4.4). Integration was achieved using the deSolve package (Soetaert et al., 2010a,b) and the VODE algorithm. RStudio (Ver. 1.4.442) was used to provide a more efficient interface with R. The optimization algorithms were called from the package nloptr (Ypma et al., 2020; <https://CRAN.R-project.org/package=nloptr>, last accessed January 16, 2020). The base model code is included in Supplementary Material 2).

RESULTS

Establishing Parameters for the Cellular Metabolism of Formaldehyde

The original DPX-PK model (Andersen et al., 2010), modified only to simulate the observed data for dG-FA adducts, predicted a hockey stick shaped curve for the production of both exogenous and endogenous dG-FA adducts with increasing concentrations of FA (Figure 3). However, in the case of dG binding, no measurable increase in the endogenous dG-adducts were observed within the concentration range examined (Lu et al., 2011). Two possibilities might explain this behavior: either the endogenous and exogenous pools of FA are not well mixed, or the free concentration of tissue acetal used in the DPX model (0.4 mM) was too high. Because it is unlikely that intracellular FA derived from endogenous sources (ie, catabolic demethylation reactions) would differ significantly from FA derived from exogenous exposure with respect to intracellular disposition and reactivity with protein and/or DNA, the total extractable tissue formaldehyde, as measured by reaction with pentafluorophenylhydrazine (Heck et al., 1982), may be overestimating the concentration of available formaldehyde (ie, the sum of free formaldehyde, FA, and FSG).

The parameters used to fit both exogenous and endogenous dG-adducts are listed in Table 1. To fit the endogenous adduct curves from Lu et al. (2011) and Yu et al. (2015; Figs. 4 and 5,

respectively), the rate of production of endogenous formaldehyde (K_p) had to be increased (from 2.45 mmol/h in the Andersen et al., 2010; PK model to 4.20 mmol/h) and the maximum rate of formaldehyde oxidase metabolism (V_{max}) increased from 2.8 mM/h used in Andersen et al. (2010) to 32.93 mM/h. As a result, the model-predicted steady-state concentration of endogenous FA (amount formaldehyde at time 0 set to steady-state FA, AFAO) using the current PK model was 0.020 mM (rather than 0.31 mM) and the basal concentration of endogenous FA bound to sulfhydryl increased from 0.057 to 0.12 mM. That is, the evidence that endogenous adduct levels

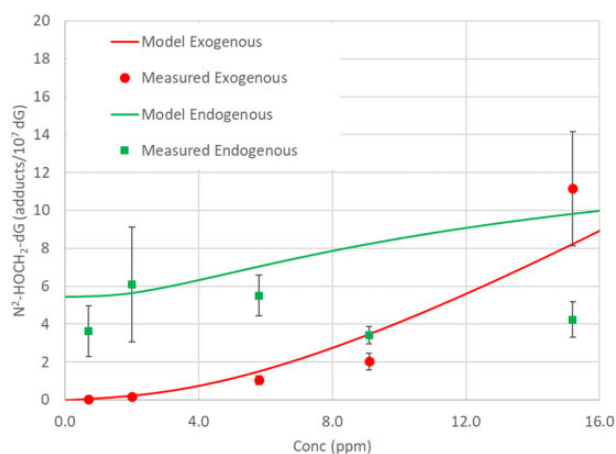


Figure 3. Predictions of the preliminary formaldehyde DNA-protein crosslinks pharmacokinetic model (Andersen et al., 2010) for endogenous (square) and exogenous (circle) formaldehyde binding to dG-DNA in rat nasal tissue after a single 6 h exposure to labeled formaldehyde concentrations of 0.7, 2, 6, 9, 10, and 15 ppm (circles: data from Lu et al., 2010; squares: data from Lu et al., 2011). This preliminary model assumed that all extractable endogenous formaldehyde (0.4 mM) is available in the tissue as formaldehyde, formaldehyde acetal, and formaldehyde glutathione thioacetal.

are not dependent on the concentration of exogenous formaldehyde requires that the kinetically available endogenous formaldehyde (ie, the sum of free formaldehyde, FA, and FSG) represents only about 75% of total extractable formaldehyde (Heck et al., 1982). The kinetically unavailable fraction is likely associated with extensive protein cross-linking that has been observed with formaldehyde.

Fitting Higher Exposure Results

The ability of the model to accurately represent levels of endogenous and exogenous FA-bound dG after single 6 h exposures to labeled formaldehyde (Lu et al., 2011) is shown in Figure 4. The current PK model captures the observed concentration-dependent transition in the relationship between inhaled FA concentrations and exogenous FA bound to dG in rat nasal tissue across the entire range of concentrations tested. The model was also consistent with the time-course data in rats (Yu et al., 2015) for a 28-day exposure to 2 ppm (Figure 5). The only parameter that differed when simulating the adduct data from the Lu et al. (2011) and Yu et al. (2015) studies was the initial (background) endogenous adduct concentration. This change was necessary since the starting value reported for background adducts differed between the 2 studies.

Fitting Lower Exposure Results

Although the current model with updated tissue metabolism parameters adequately described the adduct levels following formaldehyde exposures of 0.7 ppm and greater, predictions of adduct levels at lower exposures differed significantly from levels reported by Leng et al. (2019). To examine possible explanations for deviation from the low-dose linear relationship expected for adducts (after accounting for the higher dose non-linearity that results from the saturation of formaldehyde clearance by formaldehyde dehydrogenase in the tissue compartment), we varied the V_{maxMuc} and $KMMUC$ terms to attempt to maintain fits to the data at 0.7 ppm and above while

Table 1. Parameter Values Used in the dG-Binding PK Model for Formaldehyde.

Parameter	Process Described	Value
Unchanged from Andersen et al. (2010)		
BW	Body weight	0.3 kg
MW	Molecular weight	30.026
QPC	Ventilation rate	24.75 l/h/kg ^{3/4}
K23	Second-order association rate constant for FA and GSH	300/mM/h
K32	First-order dissociation rate constant for FSG to FA and GSH	200 h
GSH0	Initial concentration of GSH	2.0 mM
SA	Surface area ^a	16.98 cm ²
THICK	Epithelial tissue thickness ^{a,b}	0.01 cm
Parameters estimated from dG-binding studies		
K_p	Endogenous production rate of FA	4.20 mM/h
V_{max}	Maximum rate of oxidation of FA and release of GSH	32.93 mM/h
K_{21}	First-order rate constant for loss of FA	5.42/h
K_m	Affinity constant for oxidation of FA and release of GSH	0.45 mM
K_{dna}	Rate constant for binding of FA to dG in DNA	1.28×10^{-21} l/h/10 ⁷ dG
K_{rep}	Rate constant for repair of dG-bound FA	0.0063/h/10 ⁷ dG
AFA0	Initial concentration of endogenous FA	0.020 Mm
ASGO	Initial concentration of FA bound to GSH	0.12 mM
AENDDG0	Initial endogenous dG-bound FA	Lu: 3.2×10^{-21} mM Yu: 4.1×10^{-21} Mm
V_{maxMuc}	Mass cutoff from extra- to intracellular compartments	1.213×10^{-4} (mmol/h)

^aConolly et al. (2000).

^bGeorgieva et al. (2003).

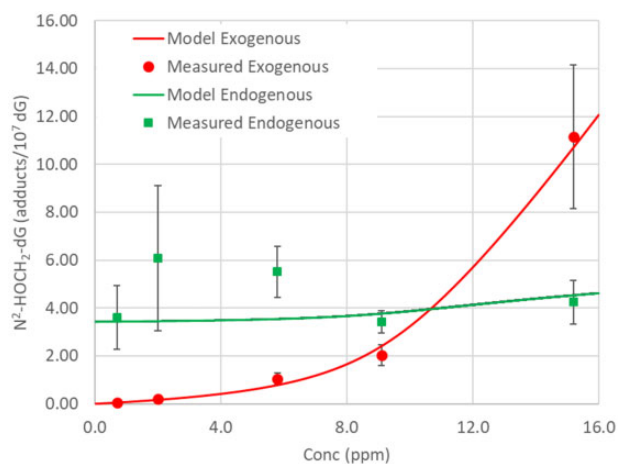


Figure 4. Predictions of the formaldehyde pharmacokinetic model for endogenous (square) and exogenous (circle) formaldehyde binding to dG in rat nasal tissue after a single 6-hour exposure to labeled formaldehyde concentrations of 0.7, 2, 6, 9, and 15 ppm (data from Lu et al., 2011). The model assumes that only a fraction of total extractable endogenous formaldehyde is available in the tissue as formaldehyde, formaldehyde acetal, and formaldehyde glutathione thioacetal.

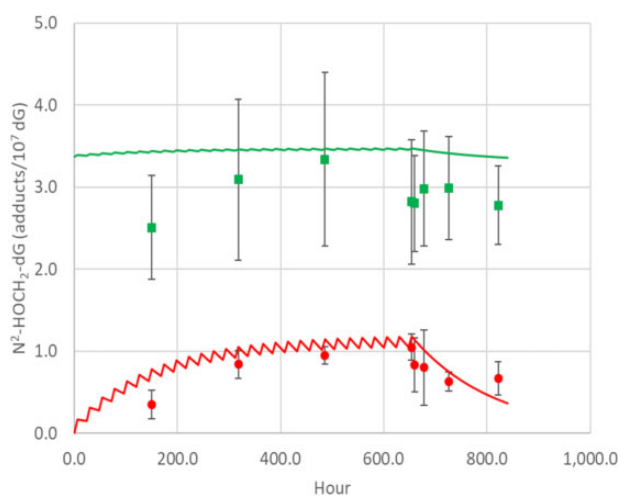


Figure 5. Formaldehyde pharmacokinetic model fit to endogenous (square) and exogenous (circle) dG binding of formaldehyde in rat nasal tissue from exposure to 2 ppm formaldehyde 6 h/day, 7 days/week, for 28 days (data from Yu et al., 2015). Model parameters (Table 1) are the same as for Figure 4, except for the basal endogenous adduct load.

predicting that there would be nonobservable levels of formaldehyde-DNA reaction products at 0.3 ppm (ie, less than the level of detection—LOD). When fitting the model to the adduct data using both a $V_{\max}M_{uc}$ term and a K_m , the fitting procedure returned extremely small values for K_m , consistent with a zero-order process. Therefore, we decided to simply fit to a term for a maximum rate of extracellular clearance (VMMUC); ie, a limiting flux rate. Below the maximum rate, no inhaled formaldehyde would reach the epithelial tissue compartment because it would be removed by extracellular clearance. Figure 6a shows the resulting fit of the revised model to the Lu et al. (2011) data for single-day 6 h exposures (circle and square symbols) while also providing consistency with the observation that adduct levels after 6 h exposures for 28 days were below the LOD in Leng et al. (2019). The 28-day simulation is represented by the dashed line (no extracellular clearance) and the dash-dot line (with

extracellular clearance). A linear plot (Figure 6b) provides a better sense of the difference between the expected adduct level at 0.3 ppm if there were no low-dose linearity associated with extracellular clearance pathways. By way of comparison, the 28-day exposure study at 0.3 ppm had adduct levels below 2 per 10^{10} dG. The predicted concentration from the low-dose-linear model with no extracellular clearance for a 28-day exposure at 0.3 ppm was 100 per 10^{10} dG.

In addition to the present model structure with low concentration extracellular clearance and the low exposure nonlinearity, we also considered whether a low capacity, zero-order elimination could be embedded in the intracellular pool of formaldehyde and fit the data throughout the full range of exposures. This alternative model structure was not able to account for the low-dose nonlinearity because the incoming formaldehyde, even at low inhaled concentrations, enters the cellular compartment with high background concentrations of endogenous formaldehyde and becomes well mixed with the cellular formaldehyde. This model structure shows linearity continuing into the low exposure region.

DISCUSSION

Model Parameters

An earlier DPX model (Andersen et al., 2010) was revised to predict measured levels of endogenous and exogenous FA-DNA reaction products as described in a series of papers (Leng et al., 2019; Lu et al., 2010, 2011; Yu et al., 2015). Simulations using parameters estimated in the earlier DPX model had predicted a hockey stick curve for endogenous FA DPX with increasing formaldehyde exposure concentrations related to saturation of tissue clearance by formaldehyde dehydrogenase. When this parameter set was used to simulate the short-term adduct results reported in recent studies, increases were expected for both endogenous and exogenous adducts. However, only increases in exogenous adducts were reported (Figure 3).

Two parameters required adjustment in order to fit the model to the new adduct data. These included both the background level of FA (AENDDG0) and of formaldehyde GSH conjugate (ASG0), the latter of which had to be decreased significantly. The free tissue FA in the absence of formaldehyde inhalation consistent with the new adduct model was 0.02 mM and the background FA-GSH conjugate was 0.12 mM. A possible explanation for requiring smaller background levels of FA and the GSH conjugate than the values measured in earlier studies relates to the method used to measure tissue formaldehyde—irreversible derivatization with pentafluorophenylhydrazine (Heck et al., 1982). This reaction complexes free and more tightly, but still reversibly bound forms of formaldehyde, and would overestimate free FA levels. The use of higher initial estimates of endogenous formaldehyde would lead to saturation of clearance by formaldehyde dehydrogenase at lower inhaled concentrations and shift the exposure-adduct curve inappropriately to the left.

Consistency With Other Measures of Response

With endogenous compounds, like formaldehyde, that have toxicity at higher exposures, there should be some range of exogenous exposures that do not produce appreciable changes in tissue concentrations (Andersen et al., 2010). With the current model for DNA-adducts, whether using extracellular clearance from the air phase or omitting it from the model, there are concentrations that would not lead to measurable increases in

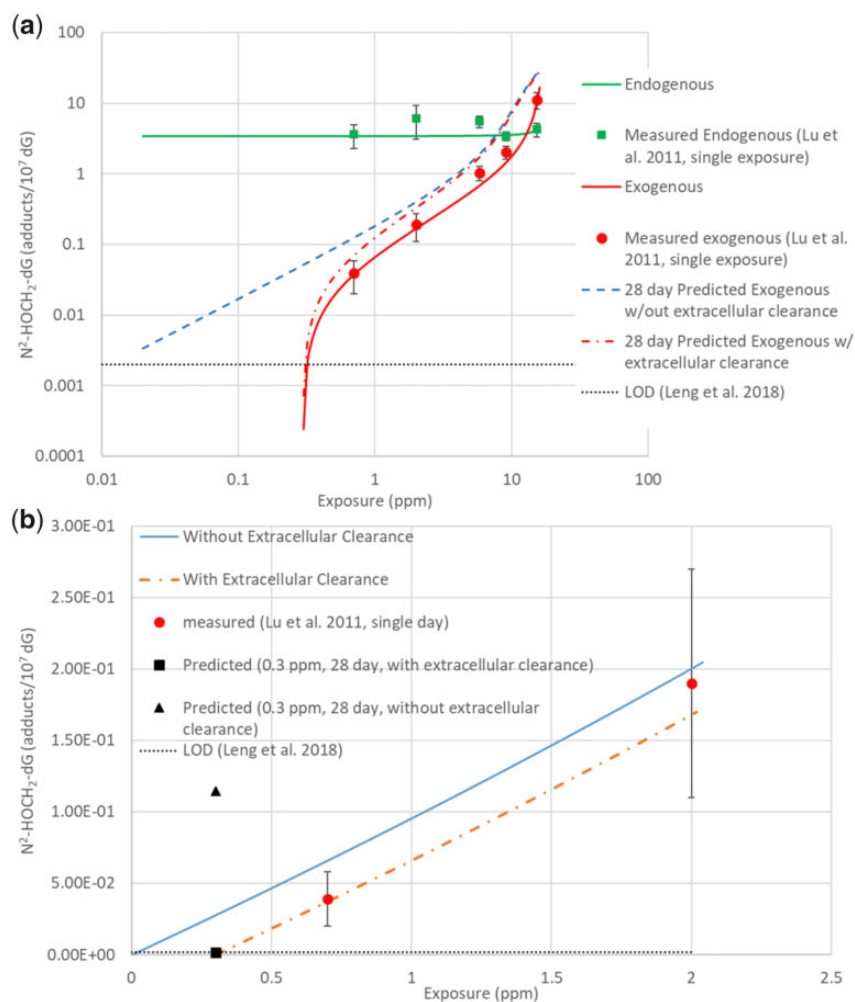


Figure 6. a, Logarithmic plot of predicted dG adducts with the current formaldehyde pharmacokinetic (PK) model that includes saturable extracellular clearance of formaldehyde (square: endogenous dG adducts; circle: exogenous dG adducts) after single 6 h exposures to labeled formaldehyde concentrations of 0.7, 2, 6, 9, and 15 ppm (Lu et al., 2011) or 28 day (6 h/day) repeated exposure without (dashed line) or with (dash-dot line) extracellular clearance. Dot-dot line is the limit of detection in the Leng et al. (2019) study. b, Linear plot of predicted exogenous dG adducts using low-dose-linear model used for Figures 4 and 5 (dashed line) and revised formaldehyde PK model that includes a saturable extracellular clearance of formaldehyde (dash-dot line) after a single 6-hour exposure to labeled formaldehyde concentrations of 0.7 and 2 ppm (Lu et al., 2011). Square is the predicted value for the 0.3 ppm, 28-day exposure in Leng et al. (2019) from the revised model that includes a zero-order clearance. Triangle is predicted value for the 0.3 ppm, 28-day exposure in Leng et al. (2019) from the same low-dose-linear model used for Figure 4. Dot-dot line is the limit of detection in the Leng et al. (2019) study.

tissue FA or tissue FA-DNA adducts. The current model structure is also consistent with nonlinear behavior reported at concentrations of approximately 2 ppm, a transition related to saturation of cellular metabolism. The absence of changes in gene expression in animals exposed to 0.7 ppm formaldehyde for 1 or 13 weeks (Andersen et al., 2010) is also consistent with regions where there would be little change in cellular FA. In these gene expression analyses, there were very few changes in gene expression in rat nasal tissue following inhalation exposure to 2 ppm formaldehyde. The only genes with significantly altered expression at 2 ppm were those related to extracellular responses to FA. Following exposure to 6 ppm, there were increases in expression of cell-cycle and DNA damage related genes—a pattern that became even more pronounced following exposure to 10 or 15 ppm. These genomic transitions are also consistent with the disproportionate increase in FA bound to DNA (ie, DPX and dG) and the nonlinear increases associated with saturation of formaldehyde dehydrogenase occurring at concentrations above 2 ppm (Andersen et al., 2010).

Interpretation of New Data

In the recent adduct study (Leng et al., 2019) conducted at lower exposures of formaldehyde (0.001–0.3 ppm), no exogenous DNA dG adducts were measured in nasal tissue after nose-only exposures for 28 consecutive days (6 h/day), with a detection limit of 2 adducts per 10^{10} dG. The expected value at 0.3 ppm based on the previous DPX model predictions (about 100 adducts per 10^{10} dG) was well-above this LOD. The results from Leng et al. (2019) were inconsistent with expectations of low-dose linearity predicted by back extrapolation of adduct formation using the parameters from analyzing adduct results from the higher dose exposures (Lu et al., 2011). This second nonlinear process in adduct formation, consistent with the work of Leng et al. (2019) at lower formaldehyde concentrations, may be related to extracellular clearance between the nasal air phase and the nasal epithelial tissues where the adducts are measured, possibly due to mucus-flow transport of mucin-bound formaldehyde away from the respiratory epithelium. To model this behavior, we included an extracellular loss pathway, initially using both a V_{max}

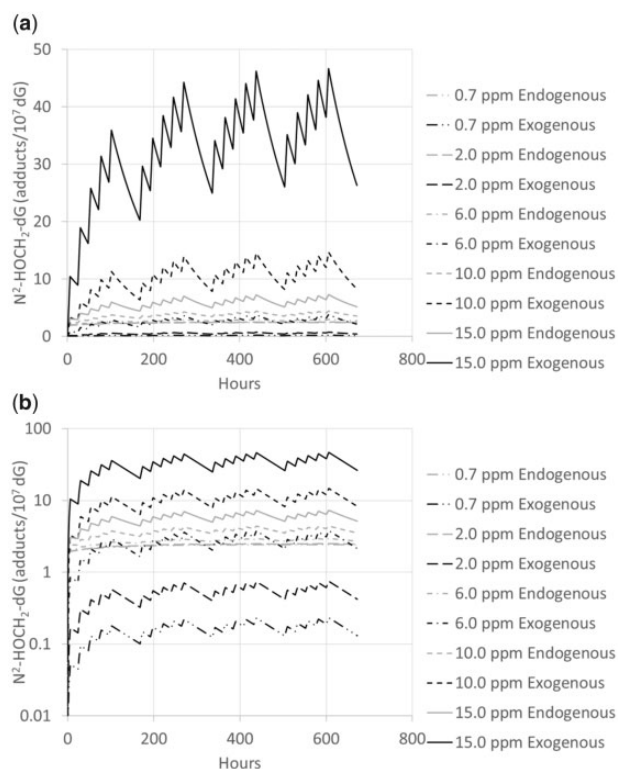


Figure 7. Model predictions (normal scale—a, log scale—b) for concentrations of endogenous and exogenous formaldehyde-dG adducts at the exposure concentrations used in the 2-year inhalation bioassays in the rat (Kerns et al., 1983; Monticello et al., 1996). Parameters estimated for the 28-day study (Yu et al., 2015) were used for this simulation. Endogenous adduct levels at 0.7 ppm (light gray-dash-dot-dot line) and 2.0 ppm (light gray-dashed line) are indistinguishable. Nasal tumors, cytotoxicity and hyperplasia were only observed at concentrations of 6 ppm and above. The modeling indicates that at the lower 2 concentrations there are far more endogenous adducts than exogenous, but at the highest concentration the exogenous adduct load can be as much as 10-fold above endogenous levels.

(called VMMUC) and a $K_m M_{uc}$ for the process. Because the change in reported adduct levels was so abrupt between 0.3 and 0.7 ppm, we could fit the loss pathway either as a zero-order process or a saturable pathway with a very small $K_m M_{uc}$. Our choice of a zero-order process in the extracellular compartment simplified the estimation of parameters and still allowed modeling the change in reported exogenous adduct levels with increasing FA concentration, with no increases in exogenous adducts predicted at 0.3 ppm (Figs. 6a and 6b). This zero-order process is consistent with the apparent low-dose nonlinearity observed in the reported data (Leng et al., 2019) and would predict a true threshold in delivered dose where no FA reaches tissue until the flux exceeds V_{max} . Implementation using a term with a binding constant for the clearance term would be consistent with penetration of some small amount of FA to the tissues at all exposures.

Another characteristic of the cellular compartment in this description of nasal tissues is the use of a single, well-mixed tissue compartment. Other processes might also affect delivery of FA to the nucleus, including uneven cellular distribution of activities of formaldehyde dehydrogenase enzymes or other clearance pathways. For instance, once in the cells, the FA has to pass through the cytoplasm and nuclear membrane before accessing DNA. None of these events prior to reaction with DNA are included in the current model structure. In addition, we did

not model specific processes within the nucleus, such as histone demethylation producing FA or locally high concentrations of clearance enzymes such as aldehyde dehydrogenase 5 (Pontel et al. 2015). FA generated within the nucleus from histone demethylation reactions would have more ready access to DNA and evade intracellular protective mechanisms. Despite these various possibilities for describing a larger set of interactions of FA in cells, we opted for parsimony—trying to be as simple as possible and still capturing the low- and high-exposure nonlinearities. We were able to achieve this goal—fitting of the full dataset using a single well-mixed cellular compartment and a precellular clearance pathway. Overall, the metabolic parameters in the tissue phase are responsible for the predictions of high-exposure nonlinearity between 2 and 15 ppm while the extracellular clearance pathway provides a high affinity, low capacity clearance for removing low concentrations of formaldehyde prior to reaching the cells.

- Using this extracellular clearance with $VMMUC = 1.213 \times 10^{-4}$ mM/h, the model predicts a highly nonlinear dose-response at low concentrations (Figs. 6a and 6b) consistent with the nondetect data from Leng et al. (2019). Nevertheless, the consistency of the revised model with the new data is not, by itself, sufficient to demonstrate the presence or nature of the low capacity, high-affinity extracellular clearance for formaldehyde. Identification of the specific pathway will be important in defining how the pathway might vary between species and its impact on risk assessments that use measures of tissue dose for estimating likely risks.

Applications of the model: Our modification and extension of the earlier formaldehyde PK modeling efforts accounts for both endogenous and exogenous dG-bound FA and should provide another computational tool to assess the dose-response for delivery of formaldehyde to epithelial tissue in the front of the nose. For example, Figures 7a and 7b show the model predictions for concentrations of endogenous and exogenous formaldehyde-dG adducts resulting from the exposure concentrations used in the 2-year inhalation bioassays in the rat (Kerns et al., 1983; Monticello et al., 1996). Parameters estimated for the 28-day study (Yu et al., 2015) were used for this simulation. In these bioassays, nasal tumors, cytotoxicity, and hyperplasia were observed following exposure of rats to concentrations of 6 ppm formaldehyde and above. Although at concentrations below 6 ppm, exogenous adducts are predicted to be well below the level of endogenous adducts, at the higher concentrations where tumors were observed, the total adduct load is predicted to be more than 10-fold above endogenous levels.

This marked difference in the ratio of endogenous to exogenous adducts in Figures 7a and 7b at lower (for instance, 6 ppm, where exogenous adducts are about equal to endogenous adducts after 28 exposure days) compared with higher exposure concentrations (ie, 15 ppm, where the exogenous adducts are about 4 times larger than endogenous adducts) arises from saturation of the cellular clearance reactions with increasing cellular concentrations of formaldehyde. Because free formaldehyde increases disproportionately with saturation of clearance, cellular concentrations of endogenous formaldehyde would also increase markedly. The expected increase in endogenous formaldehyde is reflected in Figures 7a and 7b by the increase in endogenous adducts over the 4-week simulation for 16 ppm (solid black line). No measurable increase in endogenous adducts were expected in the 4-week study at 2 ppm and none were observed (Figure 5). Although higher exposure, multiple exposure day studies could more accurately inform parameter estimation, these studies would be expensive due to the cost

mass-labeled formaldehyde and ethically questionable due to intense irritation of these exposures in the exposed rats.

The predicted adduct concentrations from this model could be used together with the available cell proliferation data (Monticello et al., 1996) in updating biologically based dose-response models for formaldehyde (Conolly et al., 2003) to evaluate the relative contributions of genotoxicity and proliferation to the nasal carcinogenicity of formaldehyde.

Our dG-binding model should also provide a useful tool for elucidating the intracellular disposition of endogenous and exogenous FA, and especially in understanding the relationship between dose-dependent transitions in FA-DNA binding (at both higher and lower exposures) and processes involved in the 2 nonlinear pathways affecting the delivered dose of formaldehyde to epithelial tissues in the front of the nose. The low concentration clearance process could be further examined in shorter term, 1- or 2-day studies of DNA-FA adduct formation that thereby help better define the changes in adduct formation and the processes involved in limiting uptake of formaldehyde at exogenous exposure concentrations below 0.7 ppm.

SUPPLEMENTARY DATA

Supplementary data are available at Toxicological Sciences online.

ACKNOWLEDGMENTS

The authors would like to thank Dr James Sherman for helpful suggestions during the preparation of this article, Dr Rory Conolly for his assistance in helping us recast the tissue PBPK model using more realistic tissue volumes and Ed Bermudez for his patience in explaining the process of tissue dissection for the nasal epithelium.

FUNDING

Foundation for Chemistry Research & Initiatives (FCRI), a 501(c)(3) tax-exempt organization established by the American Chemistry Council (ACC).

DECLARATION OF CONFLICTING INTERESTS

The authors declared no potential conflicts of interest with respect to the research, authorship, and/or publication of this article.

REFERENCES

Andersen, M. E., Clewell, H. I. I., Bermudez, E., Dodd, D. E., Willson, G. A., Campbell, J. L., and Thomas, R. S. (2010). Formaldehyde: Integrating dosimetry, cytotoxicity, and genomics to understand dose-dependent transitions for an endogenous compound. *Toxicol. Sci.* **118**, 716–731.

Conolly, R. B., Lilly, P. D., and Kimbell, J. S. (2000). Simulation modeling of the tissue disposition of formaldehyde to predict nasal DNA-protein cross-links in Fischer 344 rats, rhesus monkeys, and humans. *Environ. Health Perspect.* **108**, 919–924.

Conolly, R. B., Kimbell, J. S., Janszen, D., Schlosser, P. M., Kalisak, D., Preston, J., and Miller, F. J. (2003). Biologically motivated computational modeling of formaldehyde carcinogenicity in the F344 rat. *Toxicol. Sci.* **75**, 432–447.

Georgieva, A. V., Kimbell, J. S., and Schlosser, P. M. (2003). A distributed-parameter model for formaldehyde uptake and disposition in the rat nasal lining. *Inhal. Toxicol.* **15**, 1435–1463.

Gross, E. A., Swenberg, J. A., Fields, S., and Popp, J. A. (1982). Comparative morphometry of the nasal cavity in rats and mice. *J. Anat.* **135**(Part 1), 83–88.

Heck, H., and Casanova, M. (1999). Pharmacodynamics of formaldehyde: Applications of a model for the arrest of DNA replication by DNA-protein cross-links. *Toxicol. Appl. Pharmacol.* **160**, 86–100.

Heck, H. D., White, E. L., and Casanova-Schmitz, M. (1982). Determination of formaldehyde in biological tissues by gas chromatography/mass spectrometry. *Biomed. Mass Spectrom.* **9**, 347–353.

Kerns, W. D., Pavkov, K. L., Donofrio, D. J., Gralla, E. J., and Swenberg, J. A. (1983). Carcinogenicity of formaldehyde in rats and mice after long-term inhalation exposure. *Cancer Res.* **43**, 4382–4392.

Leng, J., Liu, C. W., Hartwell, H. J., Yu, R., Lai, Y., Bodnar, W. M., Lu, K., and Swenberg, J. A. (2019). Evaluation of Inhaled low-dose formaldehyde-induced DNA adducts and DNA-protein cross-links by liquid chromatography-tandem mass spectrometry. *Arch. Toxicol.* **93**, 763–773.

Lu, K., Collins, L. B., Ru, H., Bermudez, E., and Swenberg, J. A. (2010). Distribution of DNA adducts caused by inhaled formaldehyde is consistent with induction of nasal carcinoma but not leukemia. *Toxicol. Sci.* **116**, 441–451.

Lu, K., Moeller, B., Doyle-Eisele, M., McDonald, J., and Swenberg, J. A. (2011). Molecular dosimetry of N2-hydroxymethyl-dG DNA adducts in rats exposed to formaldehyde. *Chem. Res. Toxicol.* **24**, 159–161.

Monticello, T. M., Swenberg, J. A., Gross, E. A., Leininger, J. R., Kimbell, J. S., Seilkop, S., Starr, T. B., Gibson, J. E., and Morgan, K. T. (1996). Correlation of regional and nonlinear formaldehyde-induced nasal cancer with proliferating populations of cells. *Cancer Res.* **56**, 1012–1022.

Pontel, L. B., Rosado, I. V., Burgos-Barragan, G., Garaycochea, J. I., Yu, R., Arends, M. J., Chandrasekaran, G., Broecker, V., Wei, W., Liu, L., et al. (2015). Endogenous formaldehyde is a hematopoietic stem cell genotoxin and metabolic carcinogen. *Mol. Cell* **60**, 177–188.

Salthammer, T., Mentese, S., and Marutzky, R. (2010). Formaldehyde in the indoor environment. *Chem. Rev.* **110**, 2536–2572.

Soetaert, K., Petzoldt, T., and Setzer, R. (2010a). Solving Differential Equations in R: Package deSolve. *J. Stat. Softw.* **33**, 1–25. Available at: <http://www.jstatsoft.org/v33/i09>. Accessed January 12, 2020.

Soetaert, K., Petzoldt, T., and Setzer, R. W., (2010b). deSolve: General Solvers for Initial Value Problems of Ordinary Differential Equations (ODE), Partial Differential Equations (PDE), Differential Algebraic Equations (DAE) and Delay Differential Equations (DDE). Available at: <http://search.r-project.org/library/deSolve/html/deSolve.html>. Accessed March 3, 2020.

USEPA. (2010). Toxicological review of formaldehyde – Inhalation assessment (CAS No. 50-00-0). In *Support of Summary Information on the Integrated Risk Information System (IRIS). Volume I of IV. Introduction, Background, and Toxicokinetics*. United States Environmental Protection Agency. Washington, DC. EPA/635/R-10/002A.

Ypma, J., Johnson, S. G., Borchers, H. W., Eddebuettel, D., Ripley, B., Hornik, K., Chiquet, J., and Adler, A. (2020). Nloptr: R Interface

to NLOpt. Available at: <https://cran.r-project.org/web/packages/nloptr/index.html>. Accessed January 10, 2020.

Yu, R., Lai, Y., Hartwell, H. J., Moeller, B. C., Doyle-Eisele, M., Kracko, D., Bodnar, W. M., Starr, T. B., and Swenberg, J. A.

(2015). Formation, accumulation, and hydrolysis of endogenous and exogenous formaldehyde-induced DNA damage. *Toxicol. Sci.* **146**, 170–182.